Fractal inverse problem: an analytical approach

Eric Guérin, Eric Tosan

Fractal inverse problem: an analytical approach

Éric Guérin and Éric Tosan

January 8, 2004

1 Introduction

1.1 Fractal inverse problem

The fractal inverse problem is an important research area with a great number of potential application fields. It constists in finding a fractal model or code that generates a given object. This concept has been introduced by Barnsley with the well known *collage theorem* [Bar88]. When the considered object is an image, we often speak about fractal image compression. A method has been proposed by Jacquin to solve this kind of inverse problem [Jac92].

This problem has been studied by much authors. Generally speaking, inverse methods can be classified in two types:

- Direct methods: model characteristics are found directly. In the fractal case, very few direct methods have been proposed. In general, we have to deal with synthetic data entries. Some authors use wavelet decomposition to find frequency structures and extract IFS coefficients [Ber97, SDG95]. A method using complex moment has been experienced to work for fractal images [AKH97].

- Indirect methods: model characteristics are found indirectly. In general an optimisation algorithm is used. These methods allows to deal with more complex models and less synthetic data entries. Inverse problem for mixed IFS has been performed with genetic methods [LLVC$^+$95].

Optimisation methods used in indirect methods are generaly stochastic, because it's not possible to calculate any derivative with respect to the model parameters. In [VS99], Saupe introduced derivative property in his presentation of inverse problem. In [GTB01a, GTB02] , we developped a method based on this property for fractal approximation of curves and surfaces.

1.2 Fractal approximation

Basically, the problem of approximating the shape of objects consists in finding a model that represents a set of data points. A wide variety of representation methods have been proposed for modeling these objects[BV91]. Basically, they can be classified into three categories depending on the data source and the target application: mesh representation, parametric representation and implicit representation. For a simple visualization of smooth surfaces, the model widely used is the mesh approximation[GGN00]. When the data is issued from sensors and the model should be suitable to a CAGD use, parametric approximation seems to be well adapted using a standard model such as NURBS or B-splines[GGN00]. If the approximation should be used for a more semantic description of an object, implicit models can be chosen like superquadrics[TM91, GB93]. Each application domain has a preferred model that relies

on its specificities.

Unfortunately, these models do not recover rough surfaces, i.e. surfaces defined by continuous functions that are nowhere differentiable. In order to propose an efficient solution to the problem of rough surface approximation, we have used a parametric model based on a fractal model. In [ZT96a, ZT97b], we have proposed a *projected IFS model* for fractal curve and surfaces. This model combines a fractal classical approach – Iterative Function Systems – and CAGD classical approach – free form based on control points. These points allow an easy and flexible control of the fractal shape generated by the IFS model and provide a high quality fitting. In [GTB00, GTB01a], we have proposed an approximation method for curves based on this model. In [GTB01b], we have extended this method to surfaces. In [GTB03, Gué02], we introduced a *projected IFS tree model* to obtain a better approximation of natural surfaces and hreyscale images.

In this paper we present an analytical approach of the fractal approximation problem.

2 Modeling choice

IFS model, projected IFS model, and projected IFS tree model can be viewed as particular cases of a more general fractal modeling. This fractal modeling is based on *address functions*.

In geometric modeling parameterised shapes (curves or surfaces) are expressed as numerical argument functions, mapping from a parameterisation space ($[0,1]$ or $[0,1]^2$) to a modelisation space like $\mathcal{X} = \mathbb{R}^m$ with $m = 1, 2, 3, \ldots$. In a classical modeling approach, it is convenient to define differential properties of functions. In this way, we can construct curves or surfaces with smooth geometrical properties. In a fractal modeling approach, we want to deal with more general shapes that represent natural objects. The only property we are able to guarantee is the continuity. The set of continuous address functions can be viewed as a superset of continuous numerical argument functions.

2.1 Address functions

Address functions map from infinite words Σ^ω to a modelisation space $\mathcal{X} = \mathbb{R}^m$. We will deal with a general set of address functions: continuous functions that map from Σ^ω to $\mathcal{X}$, denoted here $C^0(\Sigma^\omega, \mathcal{X})$.

It has several advantages:

- With a unique formalism, it is possible to describe objects like curves, surfaces, images with smooth or rough aspect.
- This model allows multiresolution approach.
- Using address functions allows to extend classical analysis concepts defined on smooth shapes to rough shapes, in particular notions used for functionnal approximation.

Taking different Σ, this set includes address functions associated with IFS introduced by Barnsley and address functions associated with parameterized figures calculated from samples (curves, surfaces or digitalized figures). With a parameterisation reformulation, it includes classical free forms used in CAGD, and parameterised curves and surfaces defined with subdivision matrices [PM87, DL93]. This set includes also functions associated with images. Culik introduces similar functions defined by WFA (Weighted Finite Automaton) [CK94]. He also introduces multiresolution image as a real function $\hat{\phi} : \Sigma^* \to \mathbb{R}$ with $\Sigma = \{0, 1, 2, 3\}$ [CK95].

2.2 Continuity

The structuration in word trees permits to have a *multiresolution* approach [CK95]. The finite and infinite words set $\Sigma^\infty = \Sigma^* \cup \Sigma^\omega$ constitutes a tree for the "prefix" relation: $\alpha \leq \beta \stackrel{\text{def}}{\Leftrightarrow} \exists\gamma\ \beta = \alpha\gamma$. The root is the empty word ε, nodes are finite words and leaves are infinite words. The whole addresses set Σ^ω has an ultra-metric associated with this structure [BD85, Edg90]: $d(\sigma,\tau) = (\frac{1}{N})^{|\sigma\wedge\tau|}$ with $|\sigma\wedge\tau|$ length of $\sigma\wedge\tau$ biggest common prefix of σ and τ.

d must satisfy:

- If $\sigma \neq \tau$ then $\exists\alpha = \alpha_1...\alpha_n \in \Sigma^*$ verifying $\sigma = \alpha i\sigma'$ and $\tau = \alpha j\tau'$ with $i \neq j$, $\sigma\wedge\tau = \alpha$ and $d(\sigma,\tau) = (\frac{1}{N})^n > 0$;
- If $\sigma = \tau$ then $\sigma\wedge\tau = \sigma$ have an infinite length and $d(\sigma,\tau) = \lim_{n\to\infty}(\frac{1}{N})^n = 0$.

The balls of (Σ^ω, d) are mapping with the finite words of Σ^*:

$$B(\sigma,\varepsilon) = \alpha\Sigma^\omega = B(\sigma,\frac{1}{N^n}) \text{ with } (\frac{1}{N})^n \leq \varepsilon < (\frac{1}{N})^{n-1} \text{ and } \alpha = \sigma_1...\sigma_n$$

Because we have:

$$\begin{aligned} d(\sigma,\tau) \leq \varepsilon &\Leftrightarrow d(\sigma,\tau) \leq (\frac{1}{N})^n, \\ &\Leftrightarrow |\sigma\wedge\tau| \geq n, \\ &\Leftrightarrow \tau = \sigma_1...\sigma_n\tau'. \end{aligned}$$

ϕ is continuous means that his values are close to each other when considering deep enough nodes:

$$\phi(\sigma) \approx \phi(\tau) \text{ for } \sigma,\tau \in \alpha\Sigma^\omega.$$

The deeper α is, the more ϕ is precise.

2.3 Tabulation

This leads to the idea of *tabulating* the function ϕ, that means evaluating ϕ on finite and growing sets. Tabulation of ϕ with a resolution n is the finite familly of values: $\phi(\alpha k^\omega)$ with $\alpha \in \Sigma^n$ and $k \in \Omega \subseteq \Sigma$. This kind of tabulation can be obtained, for example, with interpolating subdivision schemes.

Remark: In the curve case $\phi(\sigma) = F(\varphi^I(\sigma))$, formal and numerical notions are equivalent:

- The address σ corresponds to the base N development of the parameter s: $\phi(\sigma) = F(s)$;
- The set $\Omega = \{0, N-1\}$ corresponds to the boundaries: $\phi(0^\omega) = F(0)$ and $\phi((N-1)^\omega) = F(1)$;
- The formal tabulation corresponds to the numerical tabulation: $\phi(\alpha'(N-1)^\omega) = \phi(\alpha 0^\omega) = F(\frac{j}{N^n})$, with $\alpha = \alpha_1...\alpha_n$ and $\alpha' = \alpha_1...\alpha_{n-1}\alpha_n - 1$ the two developments in base N of $\frac{j}{N^n}$:

$$\begin{aligned} \frac{j}{N^n} &= \sum_{i=1}^{n} \frac{1}{N^i}\alpha_i, \\ &= \varphi^I(\alpha_1...\alpha_n 0^\omega), \\ &= \varphi^I(\alpha_1...(\alpha_n - 1)(N-1)^\omega). \end{aligned}$$

2.4 Example

A simple example shows that address functions are far more general. Figure 1 illustrates the main difference between scalar argument functions and address functions. In the first case (Figure 1a), the point $\frac{1}{2}$ is a real problem, we have to choose wether the function value at this point is 0 or 1. In the second case (Figure 1b), and because $\frac{1}{2}$ has two binary expanding 01^ω and 10^ω, we can define a continuous function wich is valued for this two expandings.

The interval $[0, \frac{1}{2}]$ in the scalar case corresponds to a ball of radius $\frac{1}{2}$ in the address case: $0\Sigma^\omega = B(0^\omega, \frac{1}{2})$. In a same maner, $[\frac{1}{2}, 1]$ corresponds to $1\Sigma^\omega = B(1^\omega, \frac{1}{2})$. Note that the distance between 01^ω and 10^ω is not equal to zero:

$$d(01^\omega, 10^\omega) = 1$$

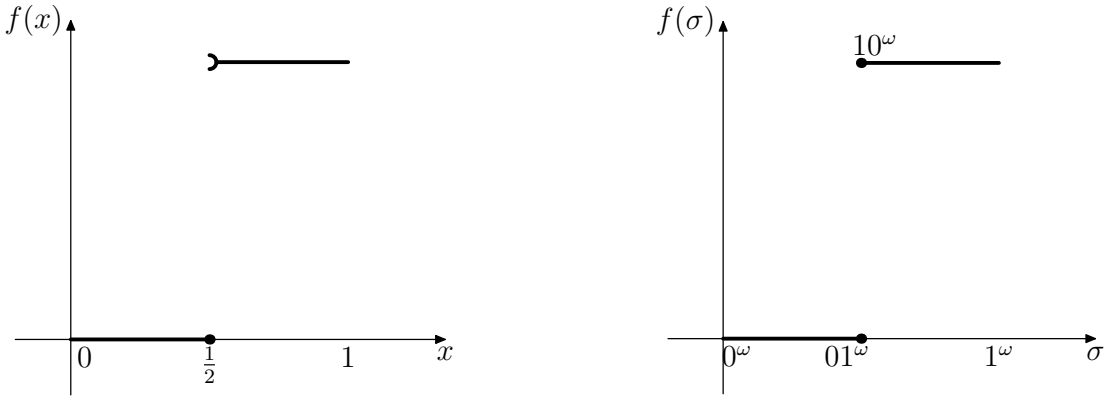

(a) Scalar argument function

(b) Address function

Figure 1: Comparison between scalar argument functions and address functions

3 Functionnal distances

We need to define a functionnal distance on address functions to be abble to estimate approximation errors. Let us suppose that $\mathcal{X}$ is a HILBERT space, for example $\mathcal{X} = \mathbb{R}^m$ with the dot product : $< x, y >= \sum_{j=1}^{m} x_i y_j$. The set $C^0(\Sigma^\omega, \mathcal{X})$, with the distance $\|\phi - \phi'\|_\infty^2 = \max_{\sigma \in \Sigma^\omega} \|\phi(\sigma) - \phi'(\sigma)\|$, is metric complete [Edg90].

However, if we want to apply classical non-linear approximation methods, we have to deal with a euclidian metric such as a square sum. This allows to calculate differentials on error functions.

To perform fractal curves and surfaces approximation, we use the following error. A level n error is evaluated with this kind of sum [CK95]:

$$D_n(\phi, \phi') = \sum_{\alpha \in \Sigma^n} \sum_{k \in \Omega} \|\phi(\alpha k^\omega) - \phi'(\alpha k^\omega)\|^2 \tag{1}$$

To define a true distance, we need to pass to the limit when n tends to infinity.

3.1 Weighted sums

To a function $f : \Sigma^\omega \to \mathbb{R}$, we associate wieghted sums:

- $S_\alpha(f)$ tabulation mean of f on a node α :

$$S_\alpha(f) = \frac{1}{M} \sum_{k \in \Omega} f(\alpha k^\omega)$$

  with $M = |\Omega|$;

- $S_n(f)$ tabulation mean of the level n:

$$\begin{aligned} S_n(f) &= \frac{1}{N^n} \sum_{\alpha \in \Sigma^n} S_\alpha(f), \\ &= \frac{1}{N^n} \sum_{\alpha \in \Sigma^n} \frac{1}{M} \sum_{k \in \Omega} f(\alpha k^\omega), \end{aligned}$$

  with $N = |\Sigma|$;

- $S(f)$ the limit, if existing, of the weighted sums serie $(S_n(f))_n$:

$$S(f) = \lim_{n \to \infty} S_n(f).$$

We have the following localisation property: $f(\sigma) \in [a, b] \Rightarrow S(f) \in [a, b]$, indeed:

$$\begin{aligned} \forall \sigma \in \Sigma^\omega \;\; f(\sigma) \in [a,b] \;\; &\Rightarrow \;\; \forall n \;\; \forall \alpha \in \Sigma^n \; \forall k \in \Omega \;\; f(\alpha k^\omega) \in [a,b], \\ &\Rightarrow \;\; \forall n \;\; \forall \alpha \in \Sigma^n \;\; S_\alpha(f) = \frac{1}{M} \sum_{k \in \Omega} f(\alpha k^\omega) \in [a,b], \\ &\Rightarrow \;\; \forall n \;\; S_n(f) = \frac{1}{N^n} \sum_{\alpha \in \Sigma^n} S_\alpha(f) \in [a,b], \\ &\Rightarrow \;\; S(f) = \lim_{n \to \infty} S_n(f) \in [a,b]. \end{aligned}$$

Because f is continuous and Σ^ω is compact, $f(\Sigma^\omega)$ is a compact of $\mathbb{R}$ and we can define:

$$a_f = \min_{\tau \in \Sigma^\omega} f(\tau), \; b_f = \max_{\tau \in \Sigma^\omega} f(\tau),$$

We have then the following double inequality: $a_f \leq S(f) \leq b_f$.

Remark: In the case of $f = F \circ \varphi^I$, we have:

$$\begin{aligned} S_n(f) &= \frac{1}{N^n} \sum_{\alpha \in \Sigma^n} \frac{1}{2}(f(\alpha 0^\omega) + f(\alpha (N-1)^\omega)), \\ &= \frac{1}{N^n} \sum_{j=0}^{N^n - 1} \frac{1}{2}(F(\frac{j}{N^n}) + F(\frac{j+1}{N^n})), \end{aligned}$$

The limit of $S_n(f)$ is a RIEMANN integral:

$$\begin{aligned} S(f) &= \lim_{n \to \infty} S_n(f), \\ &= \int_0^1 F(s) ds. \end{aligned}$$

3.2 HILBERT space of address functions

To define a euclidian metric on address functions, we introduce the following notations:

- $< \phi, \phi' >_n$ is a bilinear product sequence defined by

$$< \phi, \phi' >_n = S_n(f) \text{ with } f(\sigma) =< \phi(\sigma), \phi'(\sigma) > .$$

- $L^2(\Sigma^\omega, \mathcal{X})$ the subset of address functions in which the following limit exists:

$$< \phi, \phi' >= S(f) = \lim_{n\to\infty} < \phi, \phi' >_n .$$

Proposition 3.1 *$L^2(\Sigma^\omega, \mathcal{X})$ is a vector space.*

Proof
The function $(\phi, \phi') \to f$ with $f(\sigma) =< \phi(\sigma), \phi'(\sigma) >$ is bilinear and $\forall n$, the function $f \to S_n(f)$ is linear, the function $<,>_n$: $(\phi, \phi') \to S_n(f)$ is thus bilinear:

$$< \lambda\phi + \mu\phi', \lambda\phi + \mu\phi' >_n \;=\; \lambda^2 < \phi, \phi >_n +2\lambda\mu < \phi, \phi' >_n +\mu^2 < \phi', \phi' >_n$$

If $\phi, \phi' \in L^2(\Sigma^\omega, \mathcal{X})$, the sequence $(< \lambda\phi + \mu\phi', \lambda\phi + \mu\phi' >_n)_n$ converges, indeed we have:

$$\begin{aligned} \lim_{n\to\infty} < \lambda\phi + \mu\phi', \lambda\phi + \mu\phi' >_n &= \lim_{n\to\infty} (\lambda^2 < \phi, \phi >_n +2\lambda\mu < \phi, \phi' >_n +\mu^2 < \phi', \phi' >_n), \\ &= \lambda^2 \lim_{n\to\infty} < \phi, \phi >_n +2\lambda\mu \lim_{n\to\infty} < \phi, \phi' >_n +\mu^2 \lim_{n\to\infty} < \phi', \phi' >_n . \end{aligned}$$

Hence, $L^2(\Sigma^\omega, \mathcal{X})$ is a vector subspace of $C^0(\Sigma^\omega, \mathcal{X})$:

$$\phi, \phi' \in L^2(\Sigma^\omega, \mathcal{X}) \;\Rightarrow\; \lambda\phi + \mu\phi' \in L^2(\Sigma^\omega, \mathcal{X}).$$

□

Lemma 3.1 *$\phi \neq 0 \;\Rightarrow < \phi, \phi > > 0$.*

Proof
We have:

$$\begin{aligned} \phi \neq 0 &\Rightarrow \exists\sigma \; \phi(\sigma) \neq 0, \\ &\Rightarrow \exists\sigma \; f(\sigma) = \|\phi(\sigma)\| > 0. \end{aligned}$$

As f is continuous, there exists a ball of center σ on which f is strictly positive:

$$\exists\sigma \; \exists n \;\; (\tau \in B(\sigma, \frac{1}{N^n}) \;\Rightarrow\; f(\tau) > 0) \;\;\Rightarrow\;\; \exists\sigma \; \exists n \;\; (\tau \in \Sigma^\omega \;\Rightarrow\; f(\sigma_1 ... \sigma_n \tau) > 0)$$

Let us denote $\alpha = \sigma_1 ... \sigma_n$ and introduce the function $f_\alpha : \Sigma^\omega \to \mathbb{R}_+$ defined by $f_\alpha(\tau) = f(\alpha\tau)$, we have:

$$\begin{aligned} \forall\tau \in \Sigma^\omega \;\; f_\alpha(\tau) > 0 &\Rightarrow a_{f_\alpha} = \min_{\tau\in\Sigma^\omega} f_\alpha(\tau) > 0, \\ &\Rightarrow S(f_\alpha) \geq a_{f_\alpha} > 0 \end{aligned}$$

and:

$$S_n(f) \geq \frac{1}{N^n} \sum_{\beta \in \Sigma^n} \frac{1}{M} \sum_{k \in \Omega} f(\alpha\beta k^\omega) \quad \Rightarrow \quad S_n(f) \geq S_n(f_\alpha),$$
$$\Rightarrow \quad S(f) \geq S(f_\alpha).$$

Thus:

$$< \phi, \phi >= S(f) \geq S(f_\alpha) > 0.$$

□

Proposition 3.2 *The function* $(\phi, \phi') \rightarrow < \phi, \phi' >$ *is a dot product on* $L^2(\Sigma^\omega, \mathcal{X})$.

Proof
$<,>$ is bilinear:

$$< \lambda\phi + \mu\phi', \lambda\phi + \mu\phi' >= \lambda^2 < \phi, \phi > +2\lambda\mu < \phi, \phi' > +\mu^2 < \phi', \phi' >,$$

$<,>$ is positive definite:
We have:

$$\forall n \ < \phi, \phi >_n \geq 0 \quad \Rightarrow \quad < \phi, \phi >= \lim_{n \to \infty} < \phi, \phi >_n \geq 0.$$

The following implication: $< \phi, \phi >= 0 \Rightarrow \phi = 0$ is demonstrated by his contrary: $\phi \neq 0 \Rightarrow < \phi, \phi > \neq 0$.

□

$(L^2(\Sigma^\omega, \mathcal{X}), d_2)$ is a vector space with a euclidian like metric.
The norm and the distance associated are:

$$\|\phi\|_2 = \sqrt{< \phi, \phi >}, \ d_2(\phi, \phi') = \|\phi - \phi'\|_2$$

Proposition 3.3 $(L^2(\Sigma^\omega, \mathcal{X}), d_2)$ *is a compete metric space.*

Proof
Let $(\phi_m)_m$ be a CAUCHY sequence in $L^2(\Sigma^\omega, \mathcal{X})$, we have:

$$\lim_{m \to \infty} \|\phi_{m+1} - \phi_m\|_2 = 0 \quad \Rightarrow \quad \forall \sigma \in \Sigma^\omega \ \lim_{m \to \infty} \|\phi_{m+1}(\sigma) - \phi_m(\sigma)\| = 0.$$

To each word $\sigma \in \Sigma^\omega$ is associated a CAUCHY sequence $(\phi_m(\sigma))_m$ in $\mathcal{X}$ that has a limit.
The function ϕ_ω is then defined by:

$$\phi_\omega : \sigma \in \Sigma^\omega \mapsto \lim_{m \to \infty} \phi_m(\sigma) \in \mathcal{X}.$$

This function ϕ_ω verifies:

$$\begin{aligned}
\forall n \ < \phi_\omega, \phi_\omega >_n &= \frac{1}{N^n} \sum_{\alpha \in \Sigma^n} \frac{1}{M} \sum_{k \in \Omega} < \phi_\omega(\alpha k^\omega), \phi_\omega(\alpha k^\omega) >, \\
&= \frac{1}{N^n} \sum_{\alpha \in \Sigma^n} \frac{1}{M} \sum_{k \in \Omega} < \lim_{m \to \infty} \phi_m(\alpha k^\omega), \lim_{m \to \infty} \phi_m(\alpha k^\omega) >, \\
&= \frac{1}{N^n} \sum_{\alpha \in \Sigma^n} \frac{1}{M} \sum_{k \in \Omega} \lim_{m \to \infty} < \phi_m(\alpha k^\omega), \phi_m(\alpha k^\omega) >, \\
&= \lim_{m \to \infty} \frac{1}{N^n} \sum_{\alpha \in \Sigma^n} \frac{1}{M} \sum_{k \in \Omega} < \phi_m(\alpha k^\omega), \phi_m(\alpha k^\omega) >, \\
&= \lim_{m \to \infty} < \phi_m, \phi_m >_n
\end{aligned}$$

And we have:

$$\begin{aligned}\lim_{n\to\infty} < \phi_\omega, \phi_\omega >_n &= \lim_{n\to\infty}\lim_{m\to\infty} < \phi_m, \phi_m >_n, \\ &= \lim_{m\to\infty}\lim_{n\to\infty} < \phi_m, \phi_m >_n, \\ &= \lim_{m\to\infty} < \phi_m, \phi_m >\end{aligned}$$

$< \phi_\omega, \phi_\omega >= \lim_{n\to\infty} < \phi_\omega, \phi_\omega >_n$ exists, and ϕ_ω is in $L^2(\Sigma^\omega, \mathcal{X})$.

We have:

$$\begin{aligned}\lim_{m\to\infty} \|\phi_m - \phi_\omega\|_2^2 &= \lim_{m\to\infty}\lim_{n\to\infty} < \phi_m - \phi_\omega, \phi_m - \phi_\omega >_n \\ &= \lim_{n\to\infty}\lim_{m\to\infty} < \phi_m - \phi_\omega, \phi_m - \phi_\omega >_n\end{aligned}$$

With:

$$\begin{aligned}\lim_{m\to\infty} < \phi_m - \phi_\omega, \phi_m - \phi_\omega >_n &= \lim_{m\to\infty} \frac{1}{N^n}\sum_{\alpha\in\Sigma^n}\frac{1}{M}\sum_{k\in\Omega} < \phi_m(\alpha k^\omega) - \phi_\omega(\alpha k^\omega), \phi_m(\alpha k^\omega) - \phi_\omega(\alpha k^\omega) >_n \\ &= \frac{1}{N^n}\sum_{\alpha\in\Sigma^n}\frac{1}{M}\sum_{k\in\Omega} < \lim_{m\to\infty}\phi_m(\alpha k^\omega) - \phi_\omega(\alpha k^\omega), \lim_{m\to\infty}\phi_m(\alpha k^\omega) - \phi_\omega(\alpha k^\omega) >_n \\ &= \frac{1}{N^n}\sum_{\alpha\in\Sigma^n}\frac{1}{M}\sum_{k\in\Omega} < \phi_\omega(\alpha k^\omega) - \phi_\omega(\alpha k^\omega), \phi_\omega(\alpha k^\omega) - \phi_\omega(\alpha k^\omega) >_n \\ &= 0\end{aligned}$$

ϕ_ω is the limit of $(\phi_m)_m$ in the metric space $(L^2(\Sigma^\omega, \mathcal{X}), d_2)$. □

Proposition 3.4 *$L^2(\Sigma^\omega, \mathcal{X})$ is a* HILBERT *space.*

Proof
It is pre-hilbertian and metric complete. □

3.3 Decreasing condition

Proposition 3.5 *If ϕ verifies the following decreasing condition:*

$$\exists m \in \mathbb{N}\ \ \exists C \in \mathbb{R}_+\ \exists r \in [0,1[:\ n \geq m\ \Rightarrow\ \forall \alpha \in \Sigma^n \forall \sigma, \tau \in \Sigma^\omega\ \ \|\phi(\alpha\sigma) - \phi(\alpha\tau)\| \leq Cr^n \qquad (2)$$

then, the sequence $(< \phi, \phi >_n)_n$ converges and $\phi \in L^2(\Sigma^\omega, \mathcal{X})$.

Proof
The square difference gives:

$$\begin{aligned}f(\alpha i k^\omega) - f(\alpha k^\omega) &= \|\phi(\alpha i k^\omega)\|^2 - \|\phi(\alpha k^\omega)\|^2, \\ &= \|(\phi(\alpha i k^\omega) - \phi(\alpha k^\omega)) + \phi(\alpha k^\omega)\|^2 - \|\phi(\alpha k^\omega)\|^2, \\ &= \|\phi(\alpha i k^\omega) - \phi(\alpha k^\omega)\|^2 + 2 < \phi(\alpha i k^\omega) - \phi(\alpha k^\omega), \phi(\alpha k^\omega) > + \|\phi(\alpha k^\omega)\|^2 - \|\phi(\alpha k^\omega)\|^2, \\ &= \|\phi(\alpha i k^\omega) - \phi(\alpha k^\omega)\|^2 + 2 < \phi(\alpha i k^\omega) - \phi(\alpha k^\omega), \phi(\alpha k^\omega) > .\end{aligned}$$

Let us take $D = \|\phi\|_\infty = \max_{\sigma\in\Sigma^\omega} \|\phi(\sigma)\|$ and denote $C' = C(C+2D)$, we conclude that for $n \geq m$:

$$\begin{aligned}
|f(\alpha i k^\omega) - f(\alpha k^\omega)| &\leq \|\phi(\alpha i k^\omega) - \phi(\alpha k^\omega)\|^2 + 2\|\phi(\alpha i k^\omega) - \phi(\alpha k^\omega)\|\|\phi(\alpha k^\omega)\|, \\
&\leq (r^n C)^2 + 2(r^n C)D, \\
&\leq r^n C(r^n C + 2D), \\
&\leq r^n C(C + 2D), \\
&\leq r^n C'.
\end{aligned}$$

We have $\forall k \in \Omega\ f(\alpha k k^\omega) = f(\alpha k^\omega)$ and:

$$\begin{aligned}
\frac{1}{N^{n+1}} \sum_{\alpha\in\Sigma^n} \sum_{i\in\Sigma} f(\alpha i k^\omega) - \frac{1}{N^n} \sum_{\alpha\in\Sigma^n} \sum_{i\in\Sigma} f(\alpha k^\omega) &= \frac{1}{N^{n+1}} \sum_{\alpha\in\Sigma^n} (\sum_{i\in\Sigma} f(\alpha i k^\omega) - N f(\alpha k^\omega)), \\
&= \frac{1}{N^{n+1}} \sum_{\alpha\in\Sigma^n} \sum_{i\in\Sigma} (f(\alpha i k^\omega) - f(\alpha k^\omega)), \\
&= \frac{1}{N^{n+1}} \sum_{\alpha\in\Sigma^n} (f(\alpha k k^\omega) - f(\alpha k^\omega) + \sum_{i\neq k} (f(\alpha i k^\omega) - f(\alpha k^\omega))), \\
&= \frac{1}{N^{n+1}} \sum_{\alpha\in\Sigma^n} \sum_{i\neq k} (f(\alpha i k^\omega) - f(\alpha k^\omega)),
\end{aligned}$$

Hence, we have the upper bound:

$$\begin{aligned}
|S_{n+1}(f) - S_n(f)| &= |\frac{1}{M} \sum_{k\in\Omega} \frac{1}{N^{n+1}} \sum_{\alpha\in\Sigma^n} \sum_{i\neq k} (f(\alpha i k^\omega) - f(\alpha k^\omega))|, \\
&\leq \frac{1}{M} \sum_{k\in\Omega} \frac{1}{N^{n+1}} \sum_{\alpha\in\Sigma^n} \sum_{i\neq k} |f(\alpha i k^\omega) - f(\alpha k^\omega)|, \\
&\leq \frac{1}{M} \sum_{k\in\Omega} \frac{1}{N^{n+1}} \sum_{\alpha\in\Sigma^n} \sum_{i\neq k} r^n C', \\
&\leq \frac{1}{M} M \frac{1}{N^{n+1}} N^n (N-1) r^n C', \\
&\leq \frac{N-1}{N} r^n C'.
\end{aligned}$$

Let us denote $C" = \frac{N-1}{N} C'$, we have:

$$n \geq m \ \Rightarrow\ S_{n+1}(f) - S_n(f)| \leq r^n C".$$

The sequence $(< \phi, \phi >_n)_n = (S_n(f))_n$ is a CAUCHY sequence, it is then convergent and $< \phi, \phi >= \lim_{n\to\infty} < \phi, \phi >_n$ exists. □

4 Modelisation of rough shapes

The Hilbert space of address functions constitutes a general frame of geometric fractal modeling. One convenient way to provide address functions is the use of IFS (Iterated Function Systems). Furthermore, we will see that these functions verify the decreasing condition and then belong to $L^2(\Sigma^\omega, \mathcal{X})$.

4.1 IFS model

Introduced by BARNSLEY[Bar88] in 1988, the IFS (Iterated Function Systems) model generates a geometrical shape or an image [Jac92] with an iterative process. An IFS-based modeling system is defined by a triple $(\mathcal{X}, d, \mathcal{S})$ where [ZT96b, ZT97a]:

- $(\mathcal{X}, d)$ is a complete metric space, $\mathcal{X}$ is called *iteration space*;
- $\mathcal{S}$ is a semigroup acting on points of $\mathcal{X}$ such that: $\lambda \in \mathcal{X} \mapsto T\lambda \in \mathcal{X}$ where T is a contractive operator, $\mathcal{S}$ is called *iteration semigroup*.

An *IFS* $\mathbb{T}$ *(Iterative Function System)* is a finite subset of $\mathcal{S}$: $\mathbb{T} = \{T_0, ..., T_{N-1}\}$ with operators $T_i \in \mathcal{S}$. We note $\mathcal{H}(\mathcal{X})$ the set of non-empty compacts of $\mathcal{X}$. $\mathcal{H}(\mathcal{X})$ is a complete metric space with the HAUSDORF distance. The associated HUTCHINSON operator is:

$$K \in \mathcal{H}(\mathcal{X}) \quad \mapsto \quad \mathbb{T}K = T_0K \cup ... \cup T_{N-1}K \quad .$$

This operator is contractive in the complete metric space $\mathcal{H}(\mathcal{X})$ and admits a fixed point, called *attractor* [Bar88]:

$$\mathcal{A}(\mathbb{T}) = \lim_{n\to\infty} \mathbb{T}^n K \text{ with } K \in \mathcal{H}(\mathcal{X}) \,.$$

By introducing a finite set Σ, the IFS can be indexed $\mathbb{T} = (T_i)_{i\in\Sigma}$ and the attractor $\mathcal{A}(\mathbb{T})$ has an *address function* [Bar88, Edg90] defined on Σ^ω, the set of infinite words of Σ:

$$\rho \in \Sigma^\omega \mapsto \phi(\rho) = \lim_{n\to\infty} T_{\rho_1}...T_{\rho_n}\lambda \in \mathcal{X} \text{ with } \lambda \in \mathcal{X} \,. \tag{3}$$

Corollary 4.1 *Every address function associated with an IFS is in* $L^2(\Sigma^\omega, \mathcal{X})$.

Proof
Each IFS is by definition composed of contracting operators. To each T_i is associated a contraction factor $r_i \in [0, 1[$.
If we denote $r = \max_{i\in\Sigma} r_i$ and $C = \max_{\sigma,\tau\in\Sigma^\omega} \|\phi(\sigma) - \phi(\tau)\|$, then, the associated address function ϕ verifies:

$$\begin{aligned} \forall i \in \Sigma \;\; \forall \sigma, \tau \in \Sigma^\omega \;\; \|\phi(i\sigma) - \phi(i\tau)\| &= \|T_i\phi(\sigma) - T_i\phi(\tau)\|, \\ &\leq r_i\|\phi(\sigma) - \phi(\tau)\|, \\ &\leq r\|\phi(\sigma) - \phi(\tau)\|, \\ &\leq rC. \end{aligned}$$

By induction, it verifies the decreasing condition (2) :

$$\begin{aligned} \forall \alpha \in \Sigma^n \;\; \forall \sigma, \tau \in \Sigma^\omega \;\; \|\phi(\alpha\sigma) - \phi(\alpha\tau)\| &= \|T_{\alpha_1}...T_{\alpha_n}\phi(\sigma) - T_{\alpha_1}...T_{\alpha_n}\phi(\tau))\|, \\ &\leq r^n C. \end{aligned}$$

Then the function ϕ is in $L^2(\Sigma^\omega, \mathcal{X})$. □

4.2 IFS generalisation

Natural shapes are not strictly self-similar. Most of the time, we can see only projections of this self-similarity. To allow more flexible modeling, we introduced and used a projected IFS model [ZT96b, ZT97a].

Furthermore, natural objects are composed of heterogeneous parts. To cope with this problem, we indroduced another generalisation: projected IFS trees model [GTB03, Gué02].

4.2.1 Projected IFS model

The way to obtain projected IFS attractors is to use a barycentric metric space $\mathcal{X} = \mathcal{B}^J$:

$$\mathcal{B}^J = \{(\lambda_j)_{j\in J} \,|\, \sum_{j\in J} \lambda_j = 1\}$$

Then, the iteration semigroup is constituted of matrices with barycentric columns:

$$S_J = \{T \,|\, \sum_{j\in J} T_{ij} = 1,\, \forall i \in J\}$$

This choice leads to the generalisation of IFS attractors named *projected IFS attractors*:

$$P\mathcal{A}(\mathbb{T}) = \{P\lambda \,|\, \lambda \in \mathcal{A}(\mathbb{T})\}$$

where P is a polygon or grid of control points $P = (p_j)_{j\in J}$ and $P\lambda = \sum_{j\in J} \lambda_j p_j$. The associated address function is:

$$\varphi(\sigma) = P\phi(\sigma) = \sum_{i\in J} p_i \phi_i(\sigma)$$

In figure 2, an example of projected attractor is shown. This attractor is a curve, projected through four control points.

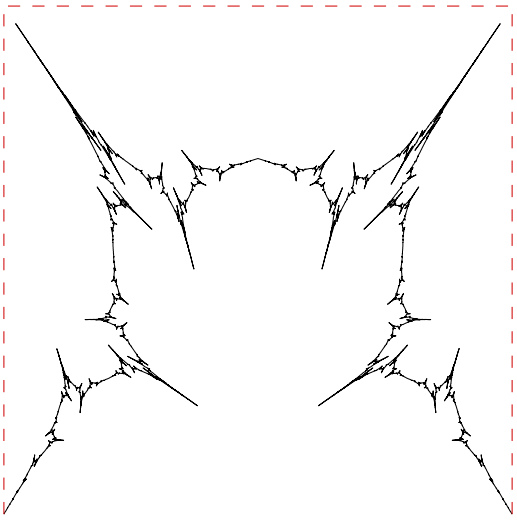

Figure 2: Example of a projected IFS curve

4.2.2 Projected IFS tree model

Let Γ be a cut of the tree $(\Sigma^\infty, \leq)$, that means a finite part of Σ^* such that each word $\sigma \in \Sigma^\omega$ admits a unique decomposition on $\Gamma \times \Sigma^\omega$:

$$\sigma = \gamma\tau \text{ with } \gamma \in \Gamma \text{ and } \tau \in \Sigma^\omega.$$

If we denote $m = \max_{\gamma\in\Gamma} |\gamma|$, then we have the following decomposition:

$$\forall n \geq m \quad \Sigma^n = \bigcup_{\gamma\in\Gamma} \gamma\Sigma^{n-|\gamma|} \text{ and } \Sigma^\omega = \bigcup_{\gamma\in\Gamma} \gamma\Sigma^\omega$$

Drawn from the families:

- of address functions $\phi^\gamma \in C^0(\Sigma^\omega, \mathcal{X}_\gamma)$,
- of affine functions $P^\gamma : \mathcal{X}_\gamma \to \mathcal{X}$.

we define a new address function with the following functionnal equation:

$$\phi(\gamma\tau) = P^\gamma \phi^\gamma(\tau)\,.$$

Proposition 4.1 *If the functions ϕ^γ verify the decreasing condition (2) then ϕ verifies this condition too.*

Proof
If we take $m = \max_{\gamma\in\Gamma} |\gamma|$ and $n \geq m$, each word $\alpha \in \Sigma^n$ can be written $\alpha = \gamma\beta$ with $\gamma \in \Gamma$ and $\beta \in \Sigma^{n-|\gamma|}$.
If we take $C = \max_{\gamma\in\Gamma} C'_\gamma C_\gamma r_\gamma^{-|\gamma|}$, and $r = \max_{\gamma\in\Gamma} r_\gamma$, we have:

$$\begin{aligned}
\|\phi(\alpha\sigma) - \phi^\gamma(\alpha\tau)\| &= \|P^\gamma\phi^\gamma(\beta\sigma) - P^\gamma\phi^\gamma(\beta\tau)\|,\\
&\leq C'_\gamma \|\phi^\gamma(\beta\sigma) - \phi^\gamma(\beta\tau)\|,\\
&\leq C'_\gamma C_\gamma r_\gamma^{n-|\gamma|},\\
&\leq C'_\gamma C_\gamma r_\gamma^{-|\gamma|} r_\gamma^{|\gamma|} r_\gamma^{n-|\gamma|},\\
&\leq C'_\gamma C_\gamma r_\gamma^{-|\gamma|} r_\gamma^{n},\\
&\leq C r^n.
\end{aligned}$$

□

Corollary 4.2 *Every address function ϕ built on address functions associated with IFS T^γ is in $L^2(\Sigma^\omega, \mathcal{X})$.*

Proof
The functions ϕ^γ are associated with IFS, that means that they verify the decreasing condition (2), and ϕ too. □

To modelise surfaces we use the address function defined by:

$$\phi(\gamma\tau) = P^\gamma \phi^\gamma(\tau)$$

and:

$$\forall\gamma \in \Gamma,\ \forall i \in \Sigma,\ \phi^\gamma(i\tau) = T_i^\gamma \phi^\gamma(\tau)\,.$$

ϕ is the address function of the compact set:

$$\phi(\Sigma^\omega) = \bigcup_{\gamma\in\Gamma} P^\gamma \mathcal{A}(\mathbb{T}^\gamma)$$

An example of heterogeneous surface is given in figure 3. Each patch of the surface can have different properties. In this example, we have mixed rough and smooth modeling together.

<table>
<tr><td colspan="2">3×3
rough</td><td>9×9
smooth</td></tr>
<tr><td>9×9
rough</td><td>9×9
rough</td><td rowspan="2">5×5
rough</td></tr>
<tr><td>3×3
smooth</td><td>5×5
smooth</td></tr>
</table>

(a) Modeling quadtree

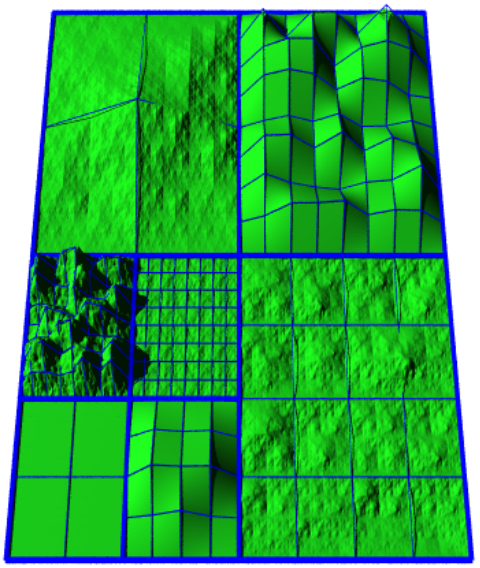

(b) Associated surface

Figure 3: Surface modeling with projected IFS quadtree

5 Approximation formulation

In the Hilbert space of address functions, optimisation problem can be expressed with the following formulation. Let φ be an address function, find $\mathbb{T}$ that minimises the error function:

$$\mathbb{T} \in \mathcal{S}^{\Sigma} \to g(\mathbb{T}) = \|\Psi(\mathbb{T}) - \varphi\|_2^2 \in \mathbb{R}_+$$

with $\Psi(\mathbb{T})$ the address function associated with $\mathbb{T}$.

To apply standard non-linear fitting methods, the function g needs to have good properties. This function is a quadratic form of Ψ. In the following, we will expose these properties.

5.1 Semigroup characterisation

We now deal with affine IFS, that means IFS defined with affine contractions in $\mathcal{X} = \mathbb{R}^m$. In this case, the contractive semigroup can be characterised. An affine operator is defined by a couple (u, L) with $u \in \mathbb{R}^m$ and L a $m \times m$ matrix:

$$Tp = u + Lp$$

The set of affine operators acting on $\mathbb{R}^m$ is a complete metric space with the following distance:

$$d(T, T') = \|u - u'\| + \|L - L'\|$$

where

$$\|L\| = \max_{\|u\|=1} \|Lu\| .$$

Proposition 5.1 *The affine contractive semigroup is an open set $\mathcal{S} = \mathbb{R}^m \times \mathcal{B}_1$ where $\mathcal{B}_1 = \{L / \|L\| < 1\}$.*

Proof
One can easily verify that $T \in \mathcal{S}$ implies its contraction:

$$\begin{array}{rcl} \exists r \in [0,1[,\, \forall p,q \in \mathbb{R}^m,\, d(Tp,Tq) \leq r d(p,q) & \Leftrightarrow & \exists r \in [0,1[,\, \forall u \in \mathbb{R}^m,\, \|Lu\| \leq r\|u\| \\ & \Leftrightarrow & \exists r \in [0,1[,\, \forall u \in \mathbb{R}^m,\, \|u\| = 1, \|Lu\| \leq r \\ & \Leftrightarrow & \max\limits_{\|u\|=1} \|Lu\| < 1 \end{array}$$

□

5.2 Analyticity

In this section, we precise property of the function:

$$\psi : \mathbb{T} \in \mathcal{S}^\Sigma \rightarrow \psi(\mathbb{T}) \in C^0(\Sigma^\omega, \mathcal{X})$$

Definition 5.1 *Let $\mathcal{S}^\Sigma$ be the set of indexed IFS $\mathbb{T} = (T_i)_{i\in\Sigma}$. Let ψ_ρ be the following function, where $\rho \in \Sigma^\omega$ is fixed:*

$$\begin{array}{rccc} \psi_\rho : & \mathcal{S}^\Sigma & \rightarrow & \mathcal{X} \\ & \mathbb{T} & \mapsto & \psi_\rho(\mathbb{T}) = \lim_{n\to\infty} T_{\rho_1} \dots T_{\rho_n} p \end{array}$$

As T_i is affine, we may decompose it in a translation vector u_i and a linear part L_i:

$$T_i p = u_i + L_i p$$

In this case, the product $T_i T_j$ gives $u_i + L_i u_j$ as translation vector and $L_i L_j$ as linear part. Then, we expand the matrix product:

$$\begin{array}{rcl} T_{\rho_1} \dots T_{\rho_n} p & = & u_{\rho_1} \\ & & +L_{\rho_1} u_{\rho_2} \\ & & +L_{\rho_1} L_{\rho_2} u_{\rho_3} \\ & & +\dots \\ & & +L_{\rho_1} \dots L_{\rho_{n-1}} u_{\rho_n} \\ & & +L_{\rho_1} \dots L_{\rho_n} p \end{array} \tag{4}$$

When n tends to infinity, p has no influence on this formula:

$$\lim_{n\to\infty} (L_{\rho_1} \dots L_{\rho_n} p) = 0$$

because L_i are linear contractions. Then $\psi_\rho(\mathbb{T})$ can be writen as a summation:

$$\psi_\rho(\mathbb{T}) = \lim_{n\to\infty} \sum_{k=1}^{n} L_{\rho_1} \dots L_{\rho_{k-1}} u_{\rho_k}$$

Proposition 5.2 *For every ρ in Σ^ω, the function ψ_ρ is analytical on $\mathcal{S}^\Sigma$.*

Proof
The function can be viewed as an expression with variables u_i, L_i. We can express the differential of ψ_ρ function:

$$\begin{array}{rcl} d\psi_\rho(\mathbb{T}) & = & du_{\rho_1} \\ & & +dL_{\rho_1} u_{\rho_2} + L_{\rho_1} du_{\rho_2} \\ & & +dL_{\rho_1} L_{\rho_2} u_{\rho_3} + L_{\rho_1} dL_{\rho_2} u_{\rho_3} + L_{\rho_1} L_{\rho_2} du_{\rho_3} \\ & & +dL_{\rho_1} L_{\rho_2} L_{\rho_3} u_{\rho_4} + L_{\rho_1} dL_{\rho_2} L_{\rho_3} u_{\rho_4} + L_{\rho_1} L_{\rho_2} dL_{\rho_3} u_{\rho_4} + L_{\rho_1} L_{\rho_2} L_{\rho_3} du_{\rho_4} \\ & & +\dots \end{array}$$

For the second order differentiation, we obtain:

$$\begin{aligned} d^2\psi_\rho(\mathbb{T}) &= 2dL_{\rho_1}du_{\rho_2} \\ &\quad + dL_{\rho_1}dL_{\rho_2}u_{\rho_3} + dL_{\rho_1}L_{\rho_2}du_{\rho_3} + L_{\rho_1}dL_{\rho_2}du_{\rho_3} \\ &\quad + \dots \end{aligned}$$

The kth differentiation is obtained the same way:

$$d^k\psi_\rho(\mathbb{T}) = \underbrace{d^k(u_{\rho_1}) + \cdots}_{a)} + \underbrace{d^k(L_{\rho_1}\dots L_{\rho_{k-1}}u_{\rho_k})}_{b)} + \underbrace{d^k(L_{\rho_1}\dots L_{\rho_k}u_{\rho_k+1}) + \cdots}_{c)}$$

As showed above, there are three cases to consider:

a) The number of factors is strictly lower than k. In this case, the kth differentiation is equal to zero.

b) The number of factors is equal to k. In this case, we have $k!$ possible choices for obtaining the product $dL_{\rho_1}\dots dL_{\rho_{k-1}}du_{\rho_k}$.

c) The number of factors is strictly greater than k. In this case, the result is a sum of mixed factors involving both variables u_i, L_i and differentials du_i, dL_i.

When evaluating at the point 0, i.e. $u_i = 0$ and $L_i = 0$, only one factor is kept. In the following expressions, du_i and dL_i have been replaced by u_i and L_i because we have considered the point 0.

$$\begin{aligned} d\psi_\rho(0)(\mathbb{T}) &= u_{\rho_1} \\ d^2\psi_\rho(0)(\mathbb{T}) &= 2\,L_{\rho_1}u_{\rho_2} \\ d^3\psi_\rho(0)(\mathbb{T}) &= 6\,L_{\rho_1}L_{\rho_2}u_{\rho_3} \\ &\dots \\ d^k\psi_\rho(0)(\mathbb{T}) &= k!\,L_{\rho_1}\dots L_{\rho_{k-1}}u_{\rho_k} \end{aligned}$$

Then, the Mac-Laurin expanding at the point 0 of the ψ_ρ function is:

$$\sum_{k=0}^{n}\frac{1}{k!}d^k\psi_\rho(0)(\mathbb{T}) = u_{\rho_1} + L_{\rho_1}u_{\rho_2} + \dots + L_{\rho_1}\dots L_{\rho_n-1}u_{\rho_n}$$

$$\begin{aligned} \sum_{k=0}^{\infty}\frac{1}{k!}d^k\psi_\rho(0)(\mathbb{T}) &= u_{\rho_1} + L_{\rho_1}u_{\rho_2} + \dots + L_{\rho_1}\dots L_{\rho_n-1}u_{\rho_n} + \dots \\ &= \lim_{n\to\infty} T_{\rho_1}\dots T_{\rho_n}\lambda \\ &= \psi_\rho(\mathbb{T}) \end{aligned}$$

The function ψ_ρ is equal to his Mac-Laurin expanding, it is analytical.□

5.3 Error estimation

In practical, this error function is evaluated on samples, that means on a finite number of values:

$$g_n(\mathbb{T}) = \frac{1}{N^n}\sum_{\alpha\in\Sigma^n}\frac{1}{M}\sum_{k\in\Omega}\|\psi_{\alpha k^\omega}(\mathbb{T}) - \varphi(\alpha k^\omega)\|^2$$

with $f(\sigma) = \|\psi_\sigma(\mathbb{T}) - \varphi(\sigma)\|^2$ error function on a value.

To perform finite exact computations, we take advantage of the fact that each transformation has a fixed point:

$$T_k c_k = c_k$$

We evaluate the function at a deep n, with $\|\alpha\| = n$. Then, the function has the form:

$$\begin{aligned} \psi_{\alpha k^\omega}(\mathbb{T}) &= T_{\alpha_1} \dots T_{\alpha_n} \phi(k^\omega), \\ &= T_{\alpha_1} \dots T_{\alpha_n} c_k. \end{aligned}$$

In this case, only polynomial computations have to be performed, g_n is a polynomial function:

$$g_n(\mathbb{T}) = \frac{1}{N^n} \sum_{\alpha \in \Sigma^n} \frac{1}{M} \sum_{k \in \Omega} \|T_{\alpha_1} \dots T_{\alpha_n} c_k - \varphi(\alpha k^\omega)\|^2$$

5.4 Resolution

We prooved the analyticity of affine IFS functions with respect to their matrix coefficients. We can now use a differential method to solve our problem. The litteral derivative is more complex to evaluate than a numerical approximation with a perturbation. The optimisation algorithm used is Levenberg-Marquardt, an improved gradient method [PFTV93].

6 Numerical examples

This section illustrates the theorical results obtained previously with three examples: function approximation, surface approximation and image compression.

6.1 Function approximation

This section will show a very simple example of numerical optimisation using affine IFS defined in $\mathbb{R}$.

6.1.1 Model overview

Transformations operate on $\mathbb{R}$:

$$\begin{aligned} T_i : \mathbb{R} &\to \mathbb{R} \\ x &\mapsto a_i x + b_i \end{aligned}$$

Each transformation is defined by two scalars. In this case, the address function is:

$$\phi(\rho) = b_{\rho_1} + a_{\rho_1} b_{\rho_2} + a_{\rho_1} a_{\rho_2} b_{\rho_3} + \dots$$

A simple serie converge to this value:

$$\phi(\rho) = \lim_{n \to \infty} B_n$$

where

$$\left\{ \begin{array}{rcl} B_1 &=& b_{\rho_1} \\ B_{i+1} &=& B_i + A_i b_{\rho_{i+1}} \text{ for } i \geq 1 \end{array} \right.$$

and

$$\left\{ \begin{array}{rcl} A_1 &=& a_{\rho_1} \\ A_{i+1} &=& A_i a_{\rho_{i+1}} \text{ for } i \geq 1 \end{array} \right.$$

6.1.2 Approximation formulation

When dealing with approximation, a common data type is an ordered list of points $(x_i, y_i)_{i=1,\dots,p}$. The value of x_i will be used to extract an address associated to the sample, whereas the value of y_i will be the target value of the address function. Let $\alpha^{(i)} = \alpha_1^{(i)} \dots \alpha_n^{(i)}$ be the N-adic expansion of $\bar{x}_i = \frac{j_i}{N^n}$ with $x_i = \bar{x}_i + \epsilon_i$ and $\epsilon_i < \frac{1}{N^{n+1}}$:

$$x_i = \sum_{j=1}^{\infty} \frac{1}{N^j} \alpha_j^{(i)}$$

Then, the approximation problem with affine IFS in $\mathbb{R}$ can be formulated. Given data entries $(x_i, y_i)_{i=1,\dots,p}$ where $x_{i+1} > x_i$, and a number of transformations N, find the IFS that minimizes the error:

$$\begin{aligned} \mathbb{T}_{opt} &= \operatorname*{argmin}_{\mathbb{T} \in \mathcal{S}^{\Sigma}} g_n(\mathbb{T}) \\ &= \operatorname*{argmin}_{\mathbb{T} \in \mathcal{S}^{\Sigma}} \frac{1}{p} \sum_{i=1\dots p} \| \psi_{\alpha_1^{(i)} \dots \alpha_n^{(i)} 0^{\omega}}(\mathbb{T}) - y_i \|^2 \end{aligned}$$

6.1.3 Results

We have tested our approximation method on several data sets, ranging from smooth curves to random data. As expected, the approximation quality depends on the number of transformations N taken.

Figure 4 shows the approximation of a cubic curve $y = 6(x - \frac{1}{2})^3$ with the method described previously. The original curve contains 1000 points. When approximating with only 2 transformations, the result is very bad. When the number of transformations becomes larger, the quality of approximation is better.

Figure 5 shows the approximation of a random function that contains 100 points. With only 5 transformations, the result is not so bad. Increasing the number of transformations leads to a better approximation. The upper limit of N is when we reach the number of data points: $N = p$. In this case, the exact reconstruction is possible.

Remark: The method used to solve the approximation problem is not global. It means that the result can be a local minimum.

6.2 Surface approximation

We want to approximate $(s, t) \in [0, 1]^2 \mapsto F(s, t) \in \mathbb{R}$ with a projected IFS tree. The model is described by two families of parameters: $(P^{\gamma})_{\gamma \in \Gamma}$ and $(\mathbb{T}^{\gamma})_{\gamma \in \Gamma}$. The value of the associated address function is:

$$\begin{aligned} \psi_{\alpha k^{\omega}}(P, \mathbb{T}) &= P^{\gamma} \psi_{\beta k^{\omega}}(\mathbb{T}^{\gamma}), \\ &= P^{\gamma} T^{\gamma}_{\beta_1} \dots T^{\gamma}_{\beta_l} c^{\gamma}_k \end{aligned}$$

The value of the sampling of F is:

$$\begin{aligned} \varphi(\alpha k^{\omega}) &= \varphi((\alpha_s k_s^{\omega}) \bullet (\alpha_t k_t^{\omega})), \\ &= F(\varphi^I(\alpha_s k_s^{\omega}), \varphi^I(\alpha_t k_t^{\omega})), \\ &= F(\frac{j_s}{N^n}, \frac{j_t}{N^n}), \\ &= z_{j_s, j_t}. \end{aligned}$$

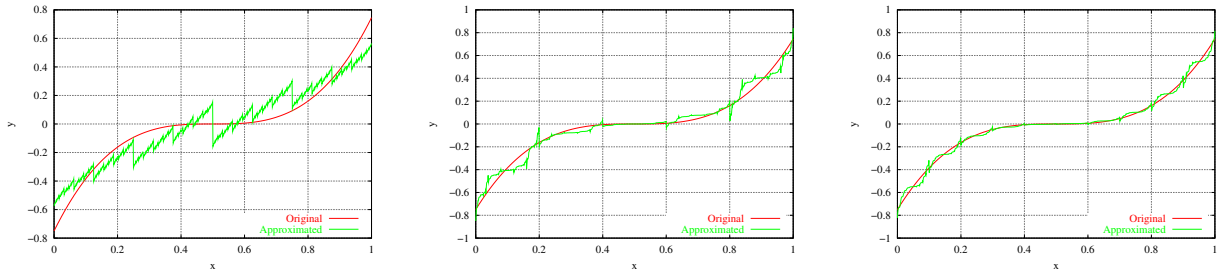

With $N = 2$ With $N = 5$ With $N = 10$

Figure 4: Approximation of a cubic polynomial curve (1000 points)

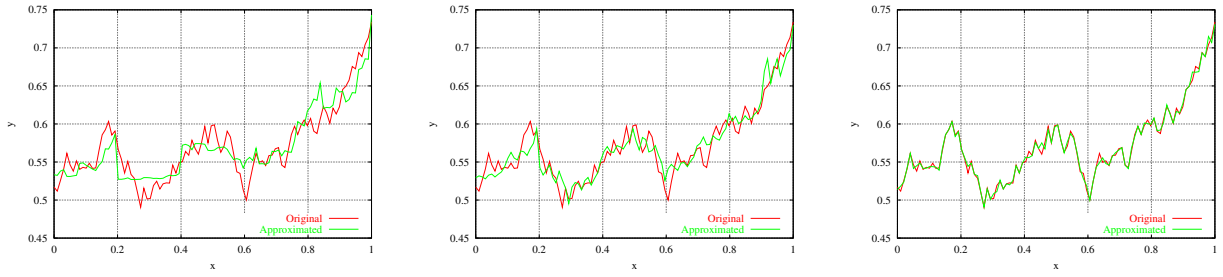

With $N = 5$ With $N = 10$ With $N = 40$

Figure 5: Approximation of a random function (100 points)

with

- $k = k_s \bullet k_t \in \Omega = \{0, N-1\} \bullet \{0, N-1\}$
- $\alpha = \alpha_s \bullet \alpha_t$ PÉANO code of the base N developpements of:

$$\begin{aligned} \frac{j_s}{N^n} &= \varphi^I(\alpha_s k_s^\omega), \\ \frac{j_t}{N^n} &= \varphi^I(\alpha_t k_t^\omega). \end{aligned}$$

Figure 6 represents the result of a surface approximation with $N = 2$. The sampling of F is an elevation grid of size 257×257. In this example, a recursive approximation method has been applied, with a simple error criterion based on a minimum PSNR value. PSNR is directly related to the definition of $g_n(\mathbb{T})$:

$$\text{PSNR}(\mathbb{T}) = 10 \log_{10}(\frac{\max}{g_n(\mathbb{T})})$$

In this example, each patch is subdivided into four independant patches while PSNR is fewer than $40dB$. Detailed method is presented in [GTB02].

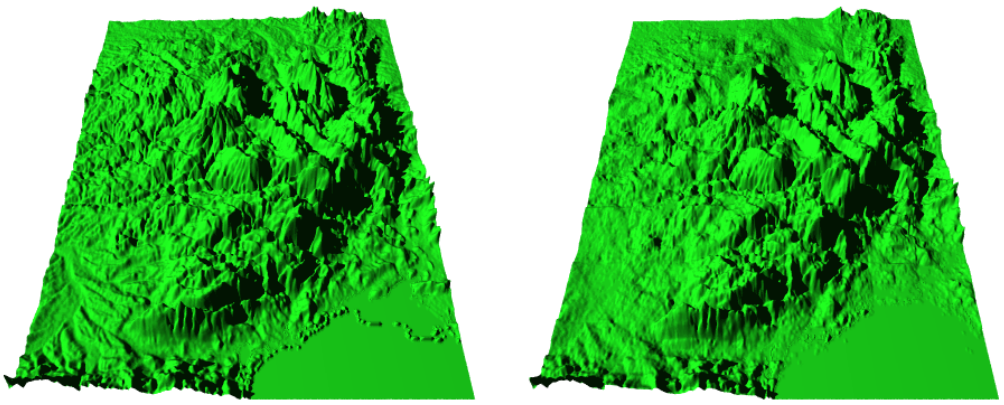

(a) Original surface (b) Approximated surface

Figure 6: Approximation of the french "Massif central" mountain

6.3 Image compression

By using the same model as surfaces, we are able to perform image compression. The difference is in the approximation method, that optimizes the rate/distortion ratio. Figure 7 shows an example of image compression. For a bit rate of $0.12bpp$, the corresponding error is PSNR=$28.3dB$, with the following classical definition of PSNR:

$$\text{PSNR}(\mathbb{T}) = 10 \log_{10}(\frac{255}{g_n(\mathbb{T})})$$

Detailed method is available in [GTB03, Gué02].

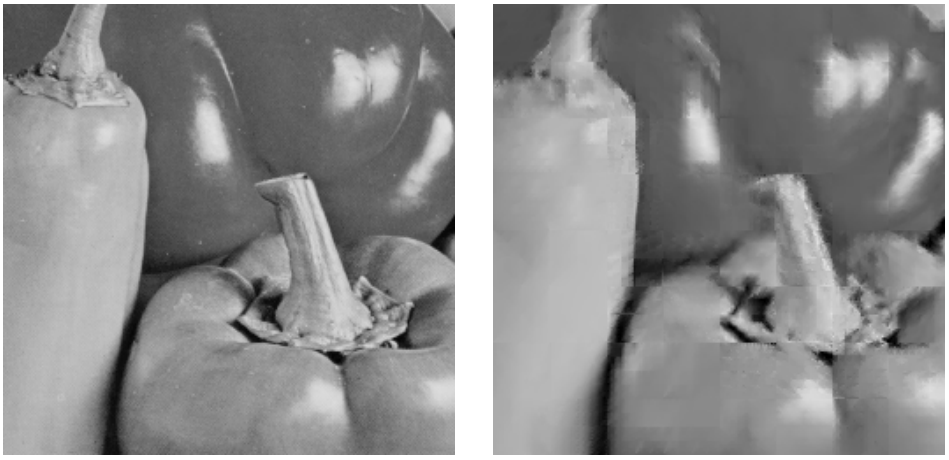

(a) Original image: portion of peppers

(b) Image compressed at $0.12bpp$, PSNR=$28.3dB$

Figure 7: Image compression example

7 Conclusion

We showed that analytical approach and methods using derivation properties can be used to perform the fractal inverse problem. This problem can be formulated as an optimisation problem in an Hilbert space. For a usefull family of fractal model based on affine IFS, the error function is analytical. Hence, the optimisation problem has a non-linear classical formulation. This result has been experienced to work practicaly on the simple case of IFS in $\mathbb{R}$. Our previous work on complex cases such as surfaces or images have a theoritical justification.

References

[AKH97] Toshimizu Abiko, Masayuki Kawamata, and Tatsuo Higuchi. An efficient algorithm for solving inverse problems of fractal images using the complex moment method. In *Proceedings of IEEE International Workshop on Intelligent Signal Processing and Communication Systems*, volume 1, pages S12.4.1–S12.4.6. November 1997.

[Bar88] Michael Barnsley. *Fractals everywhere*. Academic Press, 1988.

[BD85] M.F Barnsley and S. Demko. Iterated function systems and the global construction of fractals. *Proceeding of the Royal Society of London Ser A399*, pages 243–275, 1985.

[Ber97] K Berkner. A wavelet-based solution to the inverse problem for fractal interpolation functions. In Tricot Lévy-Véhel, Lutton, editor, *Fractals in engineering'97*, pages 81–92. Springer Verlag, 1997.

[BV91] R M Bolle and B C Vemuri. On Three-Dimensional Surface Reconstruction Methods. *IEEE Transactions on Pattern Analysis and Machine Intelligence*, 13(1):1–13, January 1991.

[CK94] K. Culik and J. Karhumäki. Finite automata computing real functions. *SIAM Journal on Computing*, 23(4):789–814, 1994.

[CK95] K. Culik and J. Kari. Inference Algorithms for WFA and Image Compression. In Yuval Fisher, editor, *Fractal Image Encoding and Compression*, pages 235–320. Springer-Verlag, 1995.

[DL93] Ingrid Daubechies and Jeffrey C. Lagarias. Two-scale difference equations II. local regularity, infinite products of matrices and fractals. *SIAM. J. Math. Anal.*, 23(4):1031–1079, July 1993.

[Edg90] Gerald A. Edgar. *Measure, Topology, and Fractal Geometry*. Springer Verlag, 1990.

[FX98] Zhigang Feng and Heping Xie. On Stability of Fractal Interpolation. *Fractals*, 6(3):269–273, 1998.

[GB93] A Gupta and R Bajcsy. Volumetric segmentation of range images of 3D objects using superquadrics models. *CVGIP: Image understanding*, 58(3):302–326, November 1993.

[GGN00] B Girod, G Greiner, and H Niemann, editors. *Principles of 3D Image Analysis and Synthesis*. Kluwer Academic Publishers, 2000.

[GTB00] Eric Guérin, Eric Tosan, and Atilla Baskurt. Fractal coding of shapes based on a projected IFS model. In *ICIP 2000*, volume II, pages 203–206, September 2000.

[GTB01a] Eric Guérin, Eric Tosan, and Atilla Baskurt. A fractal approximation of curves. *Fractals*, 9(1):95–103, March 2001.

[GTB01b] Eric Guérin, Eric Tosan, and Atilla Baskurt. Fractal Approximation of Surfaces based on projected IFS attractors. In *Proceedings of EUROGRAPHICS'2001, short presentations*, 2001.

[GTB02] Eric Guérin, Eric Tosan, and Atilla Baskurt. Modeling and approximation of fractal surfaces with projected IFS attractors. In M. M. Novak, editor, *Emergent Nature*. World Scientific, 2002.

[GTB03] Eric Guérin, Eric Tosan, and Atilla Baskurt. Fractal compression of images with projected ifs. In *PCS'2003, Picture Coding Symposium, St Malo*, April 2003.

[Gué02] Eric Guérin. *Approximation fractale de courbes et de surfaces*. Thèse de doctorat, Université Claude Bernard Lyon 1, December 2002.

[Jac92] A E Jacquin. Image coding based on a fractal theory of iterated contractive image transformations. *IEEE Trans. on Image Processing*, 1:18–30, January 1992.

[LLVC+95] Evelyne Lutton, Jacques Lévy-Véhel, Guillaume Cretin, Philippe Glevarec, and Cédric Roll. Mixed IFS : resolution of the inverse problem using genetic programming. Rapport de recherche 2631, Institut National de Recherche en Informatique et en Automatique, August 1995. Programme 5.

[PFTV93] W. H. Press, B. P. Flannery, S. A. Teukolsky, and W. T. Vetterling. *Numerical Recipes in C : The Art of Scientific Computing*, chapter Nonlinear Models. Cambridge University Press, 1993.

[PM87] H. Prautzsch and Charles A. Micchelli. Computing curves invariant under halving. *Computer Aided Geometric Design*, (4):133–140, 1987.

[SDG95] Z R Struzik, E H Dooijes, and F C A Groen. The solution of the inverse fractal problem with the help of wavelet decomposition. In M M Novak, editor, *Fractals reviews in the natural and applied sciences*, pages 332–343. Chapman and Hall, February 1995.

[TM91] D Terzopoulos and D Metaxas. Dynamic 3D models with local and global deformations: deformable superquadrics. *IEEE Transactions on Pattern Analysis and Machine Intelligence*, 13(7):703–714, July 1991.

[VS99] Edward R. Vrscay and Dietmar Saupe. Can one break the collage barrier in fractal image coding. In Dekking, Vehel, Lutton, and Tricot, editors, *Fractals : theory and applications in engineering*, pages 307–323. Springer, 1999.

[ZT96a] Chems Eddine Zair and Eric Tosan. Fractal modeling using free form techniques. *Computer Graphics Forum*, 15(3):269–278, August 1996. EUROGRAPHICS'96 Conference issue.

[ZT96b] Chems Eddine Zair and Eric Tosan. Fractal modeling using free form techniques. *Computer Graphics Forum*, 15(3):269–278, August 1996. EUROGRAPHICS'96 Conference issue.

[ZT97a] Chems Eddine Zair and Eric Tosan. Computer Aided Geometric Design with IFS techniques. In M M Novak and T G Dewey, editors, *Fractals Frontiers*, pages 443–452. World Scientific Publishing, April 1997.

[ZT97b] Chems Eddine Zair and Eric Tosan. Unified IFS-based Model to Generate Smooth or Fractal Forms. In A. Le Méhauté, C. Rabut, and L. L. Schumaker, editors, *Surface Fitting and Multiresolution Methods*, pages 335–344. Vanderbilt University Press, Nashville, TN, 1997.